

This work has been submitted to the IEEE for possible publication. Copyright may be transferred without notice, after which this version may no longer be accessible.

ArSMART: An Improved SMART NoC Design Supporting Arbitrary-Turn Transmission

Hui Chen, Peng Chen, Jun Zhou, Duong H. K. Luan, and Weichen Liu

Abstract—SMART NoC, which transmits unconflicted flits to distant processing elements (PEs) in one cycle through the express bypass, is a high-performance NoC design proposed recently. However, if contention occurs, flits with low priority would not only be buffered but also could not fully utilize bypass. Although there exist several routing algorithms that decrease contentions by rounding busy routers and links, they cannot be directly applicable to SMART since it lacks the support for arbitrary-turn (i.e., the number and direction of turns are free of constraints) routing. Thus, in this article, to minimize contentions and further utilize bypass, we propose an improved SMART NoC, called ArSMART, in which arbitrary-turn transmission is enabled. Specifically, ArSMART divides the whole NoC into multiple clusters where the route computation is conducted by the cluster controller and the data forwarding is performed by the bufferless reconfigurable router. Since the long-range transmission in SMART NoC needs to bypass the intermediate arbitration, to enable this feature, we directly configure the input and output ports connection rather than apply hop-by-hop table-based arbitration. To further explore the higher communication capabilities, effective adaptive routing algorithms that are compatible with ArSMART are proposed. The route computation overhead, one of the main concerns for adaptive routing algorithms, is hidden by our carefully designed control mechanism. Compared with the state-of-the-art SMART NoC, the experimental results demonstrate an average reduction of 40.7% in application schedule length and 29.7% in energy consumption.

Index Terms—SMART NoC, arbitrary-turn transmission, contention-minimized routing, bypassing, end-to-end latency.

I. INTRODUCTION

WITH the increasing number of processing elements (PEs) integrated into one chip, the communication between PEs becomes the bottleneck for performance improvement. Based on the modified Amdahl's law [1] which considers the effect of communication and synchronization in multi-core systems, the communication bottleneck damps the speedup gained by parallelism and computation acceleration. To support high-speed communication among PEs, network-on-chip (NoC), as a widespread communication infrastructure for large-scale many-core systems, has been refined and evolved in recent works. SMART NoC [2], which transmits unconflicted flits to distant PEs within one cycle through express long-distance bypass paths, is one of the most successful NoC designs. Experiments [2] show that if every flit is magically sent from the source to its destination by using the

single-cycle long-distance path, up to 85% application schedule length reduction can be achieved compared with state-of-the-art traditional NoCs. This is the “ideal” performance that SMART provides, with the optimistic assumption of single-cycle source-destination paths for all flits.

However, in practice, the actual SMART NoC performance is far away from the ideal case since the single-cycle long-distance path can hardly be built for all flits since only the winner of the arbitration among multiple long path setup requests can set up long-range links. If one packet is blocked by other packets, its bypass is broken which degrades the benefits gained by SMART NoC. Besides, the long-range path establishment is costly due to additional pipeline stages and broadcast links. To reduce wire and energy overhead of original SMART NoC, novel designs [3], [4], [5] are proposed. Also, researchers try to reduce contentions from the task mapping [6] and routing [7] perspectives. The first work turns to task mapping which is limited by the availability of PEs and only performs well in homogeneous systems. Peng et al. [7] try to avoid contention through XY-YX routing with intermediate nodes. However, in such design, routes for messages are not fully flexible and constrained by the number of turns. Thus, the contention issue is not fully addressed in aforementioned works. A straightforward way to significantly reduce the contentions is to relax these routing constraints and enable the data transmission of arbitrary-turn paths.

The challenge for SMART NoC to support arbitrary-turn transmission is placed by its distributed decision-making mechanism. In the start router, the route for a packet is locally computed and then a SMART-hop setup request (SSR), which carries the route information, is broadcast to the downstream routers via dedicated repeated wires to establish bypass. This local decision-making mechanism limits the routing algorithm used in SMART NoC in two aspects. (i) With the limited area constraint and deadlock requirement, the current route computation module within the SMART NoC router is rather functionally limited, resulting in that only rule-based routing strategy (e.g., XY), which is deterministic and only allows specific turns, is applied. (ii) The SSR delivery is constrained by the dedicated wires or using specific SSR network [3], which does not support SSR transmission with arbitrary-turn. Thus, even if we revise the original route compute unit and let it support arbitrary-turn transmission, e.g., using the table-based method, the constrained SSR delivery is not compatible with the arbitrary-turn transmission. To support the single-cycle long-distance transmission with arbitrary-turn, centralized or cluster-based design is needed. Also, inspired by that the optimal solution is easier to be derived based on global

W. Liu, H. Chen, J. Zhou and D. Luan are with the School of Computer Science and Engineering, Nanyang Technological University, Singapore. E-mail: ({hui.chen, liu}@ntu.edu.sg).

P. Chen is with the School of Computer Science and Engineering, Nanyang Technological University, Singapore, and also with the College of Computer Science, Chongqing University, Chongqing, China.

information instead of local information, the centralized or cluster-based method could manage NoC resource (i.e., routers and links) better.

In this article, we propose a novel NoC design based on SMART NoC [2], called ArSMART, which significantly decreases resource contentions and further fully utilizes bypass via our proposed mechanism of establishing arbitrary-turn paths. The main contributions of our article are as follows:

- 1) We develop an NoC design, ArSMART NoC, to set up single-cycle long-distance paths and support arbitrary-turn data transmission, which significantly reduces resource contentions. Specifically, ArSMART divides the whole NoC into multiple clusters where the route computation is conducted by the cluster controller and the data forwarding is performed by the bufferless reconfigurable router.
- 2) We present corresponding routing algorithms that enable ArSMART to manage NoC resources efficiently. Specifically, we conduct the route computation to generate a route before they demand at runtime, considering the real-time network state. The challenge to design routing algorithms for ArSMART is the difference of network states used in route computation and actual transmission. Our algorithms manage to minimize such impact and lessen contentions to improve NoC performance.
- 3) We implement the ArSMART design and matched routing algorithms in Gem5 [8], and conduct a full system simulation to show their effectiveness. Compared with the state-of-the-art SMART NoC, the experimental results demonstrate an average reduction of 40.7% in application schedule length and 29.7% in energy consumption.

The rest of this article is organized as follows: Section II provides examples to illustrate our motivations. Section III summarizes the notations we used in this article and presents the problem definition. The details of our design together with the proposed routing algorithms for different cases are shown in Section IV. To prove the efficiency of our proposed design, evaluations on performance, area and power are presented in Section V. Finally, Section VI discusses related works and Section VII concludes the article.

II. MOTIVATION

In this section, we motivate the benefits of supporting arbitrary-turn transmission and cluster-based resource management through the following examples.

Compared with XY routing applied in SMART NoC, arbitrary-turn transmission can fully utilize NoC resources under the same mapping strategy. Given the task graph and its mapping in Fig. 1(a), the given application is represented as a directed acyclic graph (DAG). For each node $v \in \mathcal{V}$, its task workload is indicated using the number inside the node, and for each edge $e_{u,v} \in \mathcal{E}$ from task u to task v , its message size is represented by the number beside the edge. The processing rate of different PEs is listed in the table of Fig. 1(a). Researchers proposed communication-aware task mapping algorithms [6] to minimize contentions, in which

up to 44.1% improvement in communication efficiency can be achieved by minimizing contention for SMART NoC. However, even cooperated with this task mapping algorithm, the XY routing would encounter contentions in Fig. 4(a) due to the limitation of PEs' availability. Totally, 80 time units are consumed as shown in Fig. 1(b). If arbitrary-turn routing is applied, only 60 time units are needed in Fig. 1(c).

For the heterogeneous system, arbitrary-turn routing algorithms can cooperate with computation-aware mapping to get the optimal performance for both computation and communication. With the same task graph in the previous example, we apply two mapping algorithms, the communication-aware mapping algorithm proposed in [6] and the computation-aware mapping presented in [9]. Under the XY routing, when applying computation-aware mapping, the timeline is shown in Fig. 1(d). Due to the contention, the total schedule length is 51 time units. As shown in Fig. 1(e), if the communication-aware mapping algorithm and XY routing are applied, even if no contention occurs, the total schedule length is 60 time units due to its prolonged task execution time. However, if the proposed arbitrary-turn routing and computation-aware mapping are applied, the schedule length is reduced to 31 time units, as indicated in Fig. 1(f).

Our arbitrary-turn routing design applies cluster-based resource management and removes per-router arbitration. To guarantee there is no contention during the transmission, ArSMART NoC blocks low-priority messages at the source. The benefit we can gain from such design is shown in Fig. 2. Generally, the traditional NoC router processes each flit through 5 stages [10]: route computation (RC), virtual channel allocation (VA), switch allocation (SA), switch transmission (ST) and link transmission (LT). The state-of-the-art research [11] shows that these 5 stages can be pipelined as shown in Fig. 2(a). As illustrated in Fig. 2(b), the SA stage in the SMART router contains two steps: switch allocation local (SA-L) and switch allocation global (SA-G). Given two messages T_1 and T_2 and their information as listed in Fig. 2. Since T_1 can bypass Router 2 in SMART NoC, the total transmission time is shortened compared with traditional NoC. However, since the bypass of T_1 is interrupted by T_2 , the bypass is broken and needs to be set up again. If we force T_1 to wait at the source, both messages can benefit from the long-range path, and the total time is decreased to 7 cycles. Moreover, we note that this is an extreme example, e.g., the message size is no more than 2 packets. If the path can be used for the messages consisting of more packets, the path configuration overhead is shared further.

III. PROBLEM DEFINITION

In this section, we will define the problem and the objective this article targets.

1) *Application*: An application is represented by a directed acyclic graph (DAG) $G = (\mathcal{V}, \mathcal{E})$, where \mathcal{V} is the set of the computation tasks and $\mathcal{E} \subseteq \mathcal{V} \times \mathcal{V}$ is the set of data transmission between tasks. For each node $v \in \mathcal{V}$, the task workload is represented by w_v , and for each edge $e_{u,v} \in \mathcal{E}$ from u to v , its message is represented by m_e . The set of all messages is notated using \mathcal{M} . Each message $m_e =$

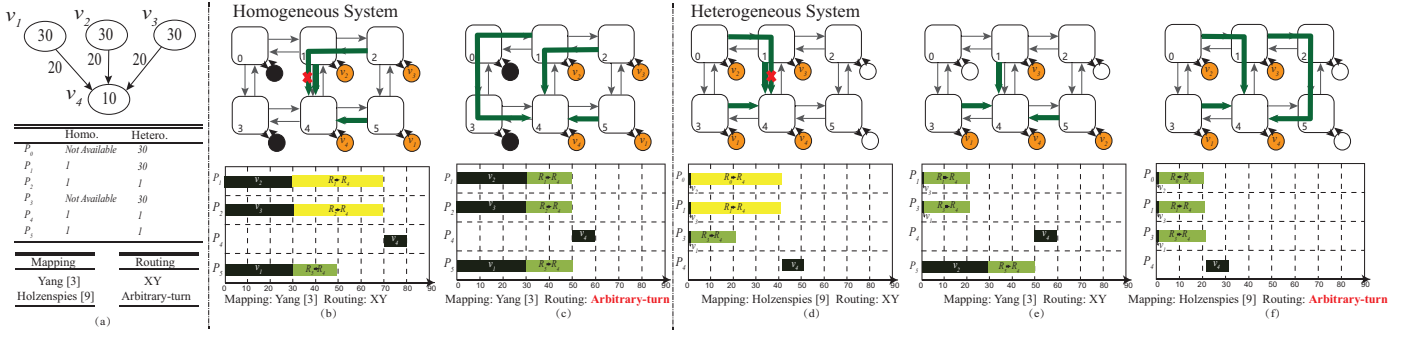


Fig. 1. Motivation examples. (a). DAG modeled application and processing rate of different PEs; (b). Communication-aware mapping and XY routing in homogeneous system; (c). Communication-aware mapping and arbitrary-turn routing in homogeneous system; (d). Computation-aware mapping and XY routing in heterogeneous system; (e). Communication-aware mapping and XY routing in heterogeneous system; (f). Computation-aware mapping and arbitrary-turn routing in heterogeneous system.

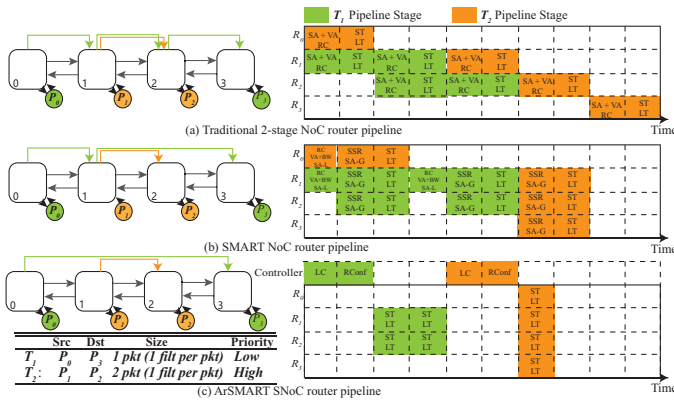


Fig. 2. Illustration of traditional, SMART and ArSMART NoC timeline.

$\{p_1, p_2, \dots, p_i, \dots, p_j\}$ consists of j packets, and each packet $p_i = \{f_1, f_2, \dots, f_i, \dots, f_k\}$ consists of k flits.

2) *Architecture*: Formally, the 2D mesh NoC-based SoC is formed of $N \times N$ PEs and routers. The PE in i^{th} row and j^{th} column is denoted by c_{ij} ($(c_{ij} \in \mathcal{C}$ and $\mathcal{C} = \{c_{1,1}, c_{1,2}, \dots, c_{N,N}\}$). The processing rate of c_{ij} is denoted by $s_{c_{ij}}$. The router in i^{th} row and j^{th} column is denoted by r_{ij} ($r_{ij} \in \mathcal{R}$ and $\mathcal{R} = \{r_{1,1}, r_{1,2}, \dots, r_{N,N}\}$).

3) *Mapping Algorithm*: Application mapping \mathcal{F} is a function from tasks \mathcal{V} to processors \mathcal{C} . $\mathcal{F}(v) = c$ represents the mapping of task v onto processor c . Based on w_v and s_c , the execution time $q_{v,c}$ for task v on processor c is estimated by $q_{v,c} = w_v / s_c$. We note that, due to the existence of branch operations, the $q_{v,c}$ value, estimated in the design time, may not be the same as the actual execution time in the run time.

4) *Routing Algorithm*: The routing algorithm is a function from messages \mathcal{M} to routers \mathcal{R} . $\mathcal{G}(m) = \gamma$ represents message m transmitting over the route γ . The route $\gamma = \{r_{src}, \dots, r_{dst}\}$ is a set of routers that forward this message from the source to the destination. In the distributed NoC system, to reduce the route computation overhead and avoid deadlock, constraints are added on the route, e.g., flits need to traverse in X direction at first and then Y direction for XY routing. We use notations \mathcal{G}_w and $\mathcal{G}_{w/o}$ to represent the routing algorithms with or without constraints. Also, we use the item “arbitrary-turn route” to notate the routing algorithm without

any constraints.

5) *Packet End-to-End Latency*: For the distributed NoC, the end-to-end latency L_{e2e} of a packet consists of head flit transmission latency L_{head} , serialization latency L_{seri} and contention latency L_{ct} , as shown in Eq. 1.

$$L_{e2e} = L_{head} + L_{seri} + L_{ct} \quad (1)$$

Generally, in traditional hop-by-hop traversal NoCs, flits are forwarded hop by hop. The end-to-end latency of a packet for traditional NoCs L_{e2e}^C can be formulated as follows.

$$L_{e2e}^C = L_r \cdot (|\gamma| - 1) + L_w \cdot |\gamma| + L_w \cdot (|f| - 1) + L_{ct} \quad (2)$$

As shown in Eq. 2, L_r and L_w are the router-stage delay and propagation delay between two adjacent routers, respectively. $|\gamma|$ represents the number of routers of the route from the source to the destination; $|f|$ refers to the number of flits of a packet. For SMART NoC, due to the bypassing of intermediate routers, the end-to-end latency L_{e2e}^S is represented by Eq. 3. Where $|ct|$ and $|limit|$ are the bypass broken overhead suffered from contention and limitation of HPC_{max} . From the formula, we find that the SMART latency is affected by contention in two aspects: the extra blocking latency and the prolonged head flit transmission latency caused by bypass break.

$$L_{e2e}^S = 2 \times (L_r + L_w) + (|ct| + |limit|) \times (L_r + L_w) + (|f| - 1) \times L_w + L_{ct} \quad (3)$$

For our proposed ArSMART NoC, since the route is configured by the controller directly, head flit carrying the route information is unnecessary, which means L_{head} used to set up route is replaced with route configuration time, L_{conf} . Then, the data can be transmitted from the source to the destination costing L_{tr} . For the contention delay, our method eliminates the contention at intermediate routers. Instead, an additional delay at the source L_{cs} is added. The latency to transmit a message using our design L_m^{ar} is represented by Eq. 4. We denote the latency without contention using $L_{w/oc}$.

$$L_m^{ar} = L_{conf} + L_{tr} + L_{cs} = L_{w/oc} + L_{cs} \quad (4)$$

Note that in our design, the path is built at message level rather than packet level. Thus, the configuration time is shared by multiple packets as $L_{conf}/|p|$. Finally, the end-to-end latency

TABLE I
NOTATIONS USED IN THIS ARTICLE

Notation	Description
$\mathcal{V}, \mathcal{E}, \mathcal{M}$	The set of tasks nodes, edges and messages.
m, p, l	The notation of message, packet and flit.
$ \cdot $	The number of elements.
\mathcal{C}, \mathcal{R}	The set of processing elements and routers.
r_{xy}	The router in x^{th} row and y^{th} column.
$q_{v,c}$	The execution time of v on c .
\mathcal{F}, \mathcal{G}	The mapping and routing algorithm.
γ_m	The route to transmit data of message m .
L	The latency related to transmission.
τ_m	The priority of message m .

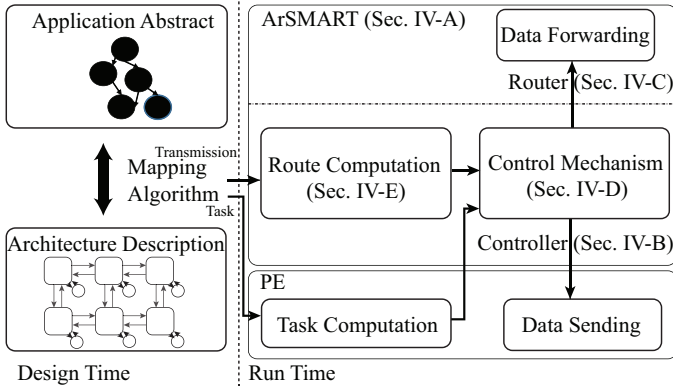


Fig. 3. Illustration of ArSMART NoC context.

of a packet for our design L_{e2e}^{ar} is represented by Eq. (5).

$$L_{e2e}^{ar} = L_{conf}/|p| + |limit| \times (L_r + L_w) + (|f| - 1) \times L_w + L_{cs}/|p| \quad (5)$$

In Table I, we summarize notations we used throughout this article. We have presented message latency of our design in 4.

The objective of our designs is to minimize the latency for each message, i.e., $Min(L_m^{ar})$. Specifically, using efficient control mechanism, we tried to minimize L_{conf} . The objective of our routing algorithm is to find the route which minimize the L_{cs} , i.e., $\arg \min_{\gamma} L_{cs}$

IV. PROPOSED ARSMART NoC

The hardware-software co-design flow of ArSMART NoC is presented in Fig. 3. For a given application abstract and specific architecture description, the mapping algorithm decides the piece of code every PE should execute. After task mapping, the task graph integrated with mapping information is generated. Such task graph briefly describes task information which includes the codes' partition and location as well as transmission information which describes the source and destination of messages. With task and transmission information, the routing computation and task computation can be conducted concurrently to cover the route computation overhead of adaptive routing algorithms.

The ArSMART NoC mainly consists of two components, router and controller. Assisted by the control mechanism, the configuration of each router generated in the controller can be

accurately executed in routers, then the data from the source can be forwarded to the destination precisely. In following subsections, we will detail our proposed design.

A. Design Overview

Fig. 4 demonstrates our proposed NoC. The whole NoC is separated into multiple clusters which consist of several routers and one cluster controller. An illustrative example of 16 routers in one cluster is given in Fig. 4(a). The cluster controller connects to every router within the cluster using a point-to-point control link as shown in Fig. 4(b). To configure inter-cluster transmission paths, each cluster controller is connected to its adjacent controllers by 16-bit wires. The link state within one cluster is collected by the cluster controller.

We note that ArSMART can be scalable to any mesh-size NoCs by applying proper cluster size and the number of clusters. However, the cluster size is limited due to the control signal distribution and transmissions it can process. The maximum distance can be traversed within one cycle is limited, i.e., 8 mm at 1 GHz [2]. If the cluster controller is placed at the center, the maximum cluster size is 8×8 . If the memory size for the controller is 10 MB and each thread consumes 10 KB, the total number of messages the controller can process is 1024, which is enough for 64 PEs.

The main process to transmit a message in ArSMART is summarized as follows. After tasks are mapped to processors, the route for one message is computed. When the route for this communication request is demanded and allowed by all required controllers, the cluster controller configures the corresponding routers directly. Then the single-cycle multi-hop bypass path is established successfully. After the transmission, the path is released and the corresponding link state is updated as free. No local arbitration is needed during this process.

B. Controller Design

The controller is responsible for route computing, link arbitration and link state updating. In this article, we do not limit the specific implementation of the controller. One possible solution is that the controller is one of the PEs. Fig. 5 demonstrates our software design for the controller.

For each message, there is one thread responsible for it. The thread id is the combination of the source, destination and the number of messages sending from the same router. Four main functions of a thread are: *route computation*, *link arbitration*, *router configuration* and *link release*. (i) Based on the source and destination information, the thread computes the route for this message. (ii) After task execution finishes, the thread checks whether this message has the highest priority among all requested links. (iii) If the checking result is true, this thread configures the routers based on the computed route. (iv) When communication finishes, the thread updates the corresponding link state. Details of these functions we will illustrate in the following sections.

The controller has a shared memory that stores the link state (i.e., busy/free). The size of shared memory equals to $|R_n| \times |ports|$, where $|R_n|$ is the number of routers in this cluster and $|ports|$ is the number of ports for each router. To ensure that every entry of shared memory in the controller is

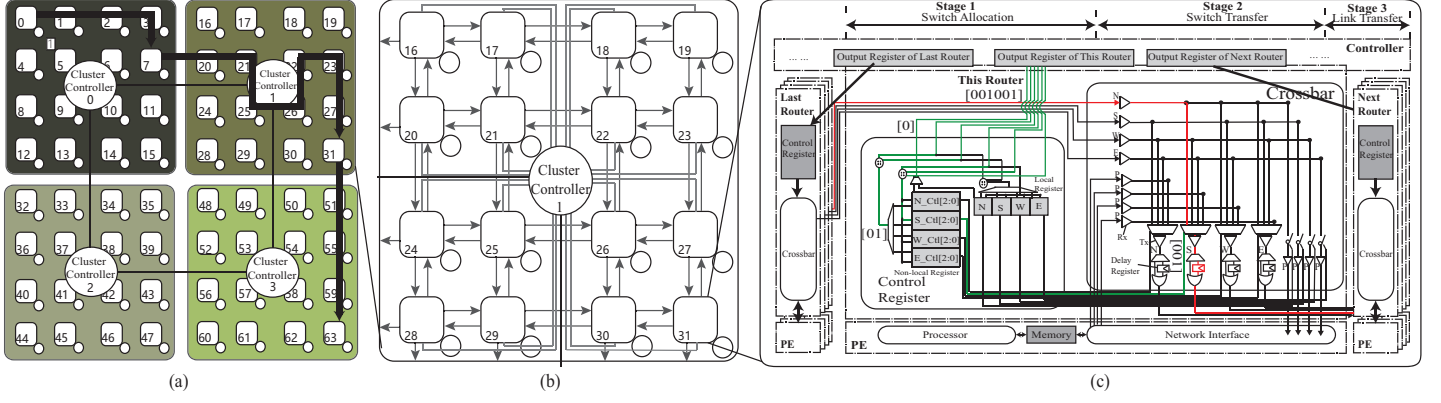


Fig. 4. ArSMART NoC Design (a). Overview of ArSMART; (b). Cluster structure; (c). Router design.

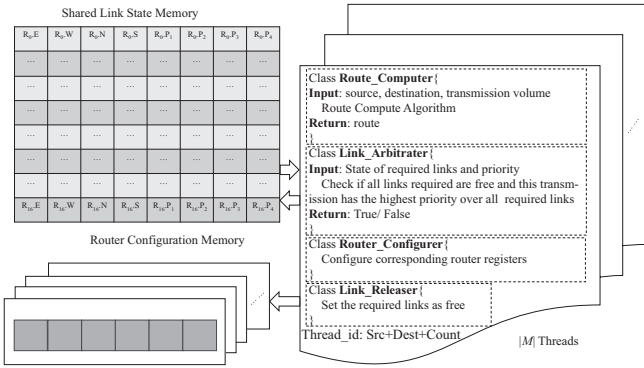


Fig. 5. Illustration of controller.

accessed by at most one thread simultaneously, we present our synchronization mechanisms (i.e., mutual exclusion). If one thread wants to occupy a link and change the link state from free to busy, it should win the priority arbitration. To perform the priority arbitration, we create a priority queue for each link. Every message requests for one link is inserted into the queue base on its priority. In our design, we apply the first-come-first-serve policy, which means the communication firstly requesting the link has the highest priority. When priority arbitration is performed, the corresponding priority queues return the first item as the result. Since only one message would win the priority arbitration for one link, the link state is updated by one thread. For low overhead, the resource arbitration is non-preemptive so that link arbitration is not conducted for one link if the required link is taken by another message already. After the message finishes, the thread would update the link state from busy to free. Since the link is occupied by one message, only one thread would change the value of the link state. We note that the cluster controller connects to every router in its cluster. Thus, configuration information can be sent to corresponding routers simultaneously.

C. Configurable Router Design

The router design is detailed in Fig. 4(c). The 6 bits configuration signal, *router-configure*, sent from controller are decoded and stored in corresponding registers as illustrated using the green lines in Fig. 4(c). The configuration register consists of two separate registers. One register with 4 entries

	Register Choose	Output Selection	Input Selection	Delay Selection
Router 31	0	0	1	0
Non-local Register: 0		N:00 S:01 W:10 E:11	1st:00 2nd:01 3rd:10 4th:11	True: 1 False:0
Router 63	1	0	0	1
Local Register:1		N:00 S:01 W:10 E:11	True: 1 False:0	X

Fig. 6. Configuration Decoding.

(3 bits for each entry), named non-local register, links the input port(s) to non-local ports (i.e., north, south, east, west ports). The other register with 4 entries (1 bit for each entry), named local register, configures the input port(s) to the local processor. ArSMART uses a 6-bit control signal to change the content of these two registers. One of the two registers is selected by the first bit. If the non-local register is chosen, the following 2 bits are used to select 1 entry and the last 3 bits are stored in that entry. The last 1 bit is used to control the delay register. Otherwise, the following 2 bits are used to choose 1 entry and only the next 1 bit is stored in that entry. The processors can send and receive data from all directions simultaneously since it connects to all non-local ports. To decrease wire delay [2], the Rx and Tx asynchronous repeaters are used. Considering the limitation of HPC_{max} , ArSMART deploys delay registers with the size of 1 flit in each input port to temporarily hold data.

In the example of transmitting data from 0 to 63, we configure router 31 and let it temporarily hold the data in delay register and forward data from N port to S port in the next cycle, as shown using the red line in Fig. 4(c). The entry 01 of the non-local register should be configured as 001, as indicated in Fig. 6. Another example is the configuration of router 63. By setting the first bit to 1, we select the local register. Since the connection between N port and local port should be built, the entry for N port is chosen and set as 1, as shown in Fig. 6. With this configuration coding, any connection between input ports and output ports can be established.

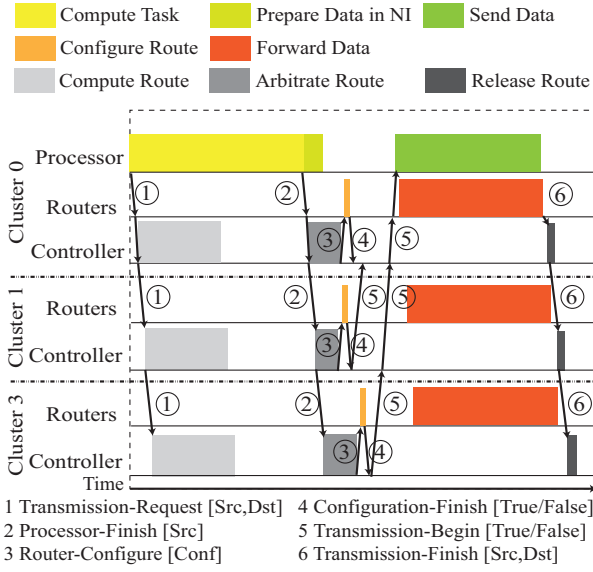


Fig. 7. Control mechanism for path establishment and release.

D. Control Mechanism

We propose a C4R (i.e., compute, check, configure, communicate and release operations) mechanism to support arbitrary-turn transmission without any local decision making. In the following, we will introduce such mechanism. Without loss of generality, we use Fig. 7 to detail the control process to transmit the message from Router 0 to 63 as illustrated in Fig. 4(a).

- **Compute.** This process computes the route for a message. After task mapping, the source and destination of messages are known. At the beginning of the task execution, for one message generated from this task, the *transmission-request* signal (12 bits) with the source and destination information is sent to the cluster controller. If more than one transmission request is submitted, the controller will process them using multiple threads. Task computation and route computation are conducted at the same time, hiding the route computation overhead. Time for route computation may be longer than task execution time, which will be discussed in the next section. In the example in Fig. 4(a), the destination is beyond the control of its cluster controller. The first controller sets a “temporary destination” at the boundary of the cluster and sends the communication request whose “temporary source” is this “temporary destination” to another cluster controller as illustrated in Fig. 7. This step would be conducted until the “temporary source” and destination are in the same cluster. The “temporary destination” is chosen randomly among the available boundary routers r_b with $r_{src_x} \leq r_{b_x} \leq r_{dst_x}$ and $r_{src_y} \leq r_{b_y} \leq r_{dst_y}$. In the example, router 7 and 31 are boundary routers. Considering the limitation of HPC_{max} , flits would latch router(s) whose hop count from the source or “temporary source” is multiple times of HPC_{max} and continue to transmit in the next cycle. Due to the concern about HPC_{max} , flits should latch boundary routers to let the count of hops for other clusters start from 0.

- **Check.** A message is eligible to transmit if and only if it can win all required links. The processor sends the *processor-finish*

(6 bits) which includes the source information to the controller as long as it finishes task execution. The transmission path for one message is exclusive, meaning that this path cannot be used by other messages simultaneously. For one message, the controller checks whether this message has the highest priority among all requested links. If the transmission is beyond the cluster, the cluster needs to forward the *processor-finish* request to other corresponding clusters. The controller only checks links within its cluster. In Fig. 4(a), controller 0 checks links used to transmit data from router 0 to 7 and the link connected to the east port of router 7. Note that if one message finds one link it needs is taken by another message, it would not request any links along its route until that message ends the transmission and release the path.

- **Configure.** If all required links are available after the “check” process, routers along the assigned path are configured by *router-configure* signal (6 bits) which we have discussed previously. For the inter-cluster case, the corresponding cluster controller(s) would configure routers if the checking result is true. Since the cluster controller connects with all routers, it can send the configuration information to all related routers simultaneously. In Fig. 4(a), controller 1 gets the true result at first, and then it configures router 20, 21, 25, 26, 22, 23, 27, 31 within one cycle. After routers finish the configuration, they send the *configuration-finish* signal (1 bits) to its cluster controller. We note that the case that more than one message configures the same router at the same time exists. However, such additional delay caused by router configuration is limited since this case rarely happens. Also, since there are 5 input ports and 5 output ports only, at most 5 cycles are needed to configure a router. Updating the link state promptly is required in our system. Before routers are configured by the controller, corresponding link states are updated as busy, so that the other messages cannot transfer data along this path.

- **Communicate.** After routers within the cluster are configured correctly, the controller sends the *transmission-begin* signal (1 bits). In the inter-cluster case, the local cluster would send the *transmission-begin* signal to the source cluster. The source cluster sends the *transmission-begin* signal to the processor if and only if it collects all *transmission-begin* signals from required clusters. In Fig. 4(a), the controller 0 sends the *transmission-begin* signal to the source PE after collecting *transmission-begin* signals from controller 1 and 3. Then the source PE begins to send data.

- **Release.** After router 0 transmitting the last flit, the links from router 0 to router 63 should be released. In the first cycle, router 0 sends the *transmission-finish* signal (12 bits) with the source and destination of this message to cluster controller. After the cluster controller receives this signal, it checks this transmission beyond this cluster so it forwards the *transmission-finish* to other corresponding cluster controllers (cluster 1 and cluster 3). Finally, all related controllers update their link state correctly.

In our system, since the route is configured by the controller directly, head flit is unnecessary, which means L_{head} used to set up the path is replaced by route configuration time, L_{conf} . The route configuration time is $Max(0, 2 \times (L_{cn} + L_{rc}) + L_{rls} - L_{pre})$, where L_{cn} is delay cycles to coordinate clusters

this path involves in; L_{rc} refers to delay cycles caused by router configuration and release. The maximum L_{rc} is 5 as we discussed before; L_{pre} is the data preparation cycles in NI. L_{conf} can be overlapped by L_{pre} . For a given path, the maximum configuration time can be computed by: $2 \times (|cn| + 5) + |cn|$, where $|cn|$ is the number of clusters this path involves in.

E. Routing Algorithm

We have presented our C4R transmission mechanism in the previous section. To fully utilize the NoC resources, we propose the corresponding routing algorithms. As mentioned before, we advance the route computation to the start of task execution to cover the route computation overhead. Note that, if too many messages are added to the task graph, the competition for the resource is inevitable. Instead of competing at intermediate routers, blocking the low-priority transmission at the source can separate different transmissions without any extra delay. We try to decrease such blocking delay at the source using our routing algorithms.

Generally, due to the existence of branch operations, the task execution time is unknown beforehand, as described in [12], and only the source and destination of messages are given. Suppose we can estimate the message size $|m|$ at the design time, like the case shown in [13]. Without knowing the exact transmission start time, we use a greedy strategy to compute the proper route for each message. The objective of the greedy strategy can be customized to meet different needs.

At the routing algorithm start time point t , we use \mathcal{M}_t to denote the set of messages which have been assigned routes and have not completed their transmission (i.e., are transmitting or waiting for transmission). In our algorithm, we only consider messages in \mathcal{M}_t since the other messages either are uncertain in route so that contention cannot be computed or have finished so that have no influence on the current network state.

For a message m_i , our algorithm try to find a route γ which minimizes the estimation upper bound of the blocking latency which suffers from messages in \mathcal{M}_t . In Theorem 1, we prove that the upper bound of blocking latency at the source m_i suffers from m_j ($j \neq i, m_j \in \mathcal{M}_t$) is $L_{w/oc_{m_j}}$.

Theorem 1. *Given a message m_i , the blocking latency at the source that m_i suffers from m_j ($\gamma \cap \gamma_{m_j} \neq \emptyset, j \neq i, m_j \in \mathcal{M}_t$) along γ , $L_{cs_{m_i \leftarrow m_j, \gamma}}$, is upper-bounded by:*

$$L_{cs_{m_i \leftarrow m_j, \gamma}} \leq L_{w/oc_{m_j}}$$

Proof. If $\gamma \cap \gamma_{m_j} = \emptyset$, m_i is not influenced by m_j and $L_{cs_{m_i \leftarrow m_j}} = 0$.

(i) $\tau_{m_j} < \tau_{m_i}$: If m_j starts transmission early than m_i , m_i has to wait until m_j ends its transmission and $L_{cs_{m_i \leftarrow m_j, \gamma}} \leq L_{w/oc_{m_j}}$. If m_j requests links late or at the same time as m_i , since $\tau_{m_j} < \tau_{m_i}$, m_i does not be influenced by m_j .

(ii) $\tau_{m_j} \geq \tau_{m_i}$: the maximum blocking latency at the source m_i suffers from m_j equals $L_{e2e_{m_j}}$, where $L_{e2e_{m_j}} = L_{w/oc_{m_j}} + L_{cs_{m_j}}$. As illustrated in our control mechanism, if m_j is blocked by another message, it ends the request for all links until that message ends its transmission. Thus, such indirect contention does not influence m_i and $L_{cs_{m_j}}$ does not

lengthen $L_{cs_{m_i \leftarrow m_j, \gamma}}$. Finally, $L_{cs_{m_i \leftarrow m_j, \gamma}} \leq L_{w/oc_{m_j}}$. The theorem is proved. \square

Theorem 2. *Given a set of messages \mathcal{M}_t , for m_i , the estimated delay at the source along the route γ , $E(L_{cs_{m_i, \gamma}})$ is upper-bounded by:*

$$E(L_{cs_{m_i, \gamma}}) \leq \sum_{m_j \in S} L_{w/oc_{m_j}}, \text{ where } S = \{m_j | \gamma \cap \gamma_{m_j} \neq \emptyset, j \neq i, m_j \in \mathcal{M}_t\}$$

Proof. $E(L_{cs_{m_i, \gamma}}) = \sum_{m_j \in S} P(m_i \leftarrow m_j, \gamma) L_{cs_{m_i \leftarrow m_j, \gamma}}$, where $P(m_i \leftarrow m_j, \gamma)$ is the probability m_j and m_i compete for the one or more links along γ at the same time, $L_{cs_{m_i \leftarrow m_j, \gamma}}$ is the blocking time m_i suffers from m_j along γ . Since $P(m_i \leftarrow m_j, \gamma) \leq 1$ and $L_{cs_{m_i \leftarrow m_j, \gamma}} \leq L_{w/oc_{m_j}}$, as illustrated in Theorem 1, $E(L_{cs_{m_i, \gamma}})$ is upper-bounded by $\sum_{m_j \in S} L_{w/oc_{m_j}}$. The theorem is proved. \square

Based on Theorem 2, the upper bound of delay at source for one message along the route γ is the total transmission time without blocking of all messages along this route. The transmission time without blocking of message m is $L_{w/oc} = L_{conf} + L_{tr}$, where $L_{tr} \propto |m|$. Since L_{conf} is relatively fixed and small, $L_{w/oc} \propto |m|$, the size of message m . Together with Theorem 2, $E(L_{cs_{m_i, \gamma}}) \propto \sum_{m_j \in S} |m_j|$, where $S = \{m_j | \gamma \cap \gamma_{m_j} \neq \emptyset, j \neq i, m_j \in \mathcal{M}_t\}$. As mentioned before, we suppose that the message size $|m|$ is estimated at the design time, like the case shown in [13]. For a message m_i , we compute the $\sum_{m_j \in S} |m_j|$, where $S = \{m_j | \gamma \cap \gamma_{m_j} \neq \emptyset, j \neq i, m_j \in \mathcal{M}_t\}$, as the cost of a candidate route γ . Among all candidate routes, we choose the route with the minimum cost using Algorithm 1. Specifically, we initialize the cost matrix in Line 2-4. For a vertex in cost matrix, we compute the upper bound of delay estimation for this vertex and its neighbor by accumulating the message size of all messages along this route, as indicated in Line 11. Then, the cost matrix is updated by checking whether the total cost can be shortened after adding the delay, shown in Line 12-13. The matrix update will end until reaching the destination in Line 8-9. Finally, we go through the previous nodes and return the route in Line 14-17.

• Improved Routing Algorithm for Time-Triggered Case

After task mapping, besides the source, destination and message size, the execution time q can also be known, as described in [14]. This is common in digital signal processing, 4G and matrix multiplication. Also, in the time-triggered real-time system [15], the activities are initiated periodically at predetermined points. With the execution time q provided, we can compute the route and transmission period for messages accurately by loading the accurate link state of a particular period, as shown in Algorithm 2. When a task v is mapped onto a core at time point t , its messages' initialized start time t_{start} is given in the time-triggered case. If no contention occurs during the transmission, the end time of the message is $t_{start} + L_{w/oc}$. Since $L_{w/oc} = L_{conf} + L_{tr}$, where L_{conf} is upper bounded by $2 \times (|cn| + 5) + |cn|$ and L_{tr} is computed by $|m| \times |p| \times (|f| - 1) \times L_w + |limit| \times (L_r + L_w)$, the upper bound of $L_{w/oc}$, $Max(L_{w/oc})$ can be computed. For one message, we compute the initialized start time and the maximum non-

Algorithm 1: Algorithm for General Case

Input: An unassigned message m ;
Output: Route γ ;

```

1 create vertex set  $Q$ ;
2 for each vertex  $v$  in  $\mathcal{R}$  do
3    $cost_v = inf; prev_v = inf; Q.enqueue(v)$ ;
4  $cost_s = 0$ ;
5 while  $Q \neq \phi$  do
6    $u$  is vertex in  $Q$  with the least  $cost_u$ ;
7    $Q.dequeue(u)$ ;
8   if  $u$  is destination then
9     break;
10  for each neighbor  $v$  of  $u$  do
11     $delay = computeCost(v, u)$ ;
12    if  $cost_v > cost_u + delay$  then
13       $cost_v = cost_u + delay; prev_v = u$ ;
14 if  $prev_{dest}$  is defined or  $u = source$  then
15   while  $u$  is defined do
16      $\gamma.push(u); u = prev_u$ ;
17 Return  $\gamma$ ;
```

contention end time in Line 1 and Line 2. The reservation list is used to save routes for all unfinished messages and their transmission periods. By checking transmission periods stored in the reservation list, the network state with available links in that period is generated in Line 5. In this article, we use Dijkstra's algorithm, in Line 6, to find the shortest path within a specific period. In this period, if data can be transmitted from source to destination in such network graph, route information and this period are inserted into the reservation list in Line 7-9. Otherwise, since links are released if and only if the transmission finishes, the algorithm tries the next finishing time point until it finds an available route in Line 11-13.

Algorithm 2: Algorithm for Time-Triggered Case

Input: An unassigned message m , route reservation list RL ;
Output: Route γ and transmission period $[t_1, t_2]$;

```

1  $t_1 = initialStartTime$ ;
2  $t_2 = t_1 + max(L_{w/oc})$ ;
3  $\gamma = \phi$ ;
4 while (1) do
5    $\mathcal{G} = loadGraph(RL, t_1, t_2)$ ;
6    $\gamma = findRoute(m, \mathcal{G})$ ; //Find route from  $r_{src}$  to  $r_{dst}$ ;
7   if ( $\gamma \neq \phi$ ) then
8      $RL.insert(\gamma, t_1, t_2)$ ;
9     Return  $\gamma$  and  $[t_1, t_2]$ ;
10  else
11    //Find the next time point when a route is released;
12     $t_1 = nextRelease(t_1, ReverseList)$ ;
13     $t_2 = t_1 + max(L_{w/oc})$ ;
```

Finally, we analyze the time complexity of these two route algorithms. For the first routing algorithm, the total number of loops equals $|\mathcal{R}|$. Inside it, minimum finding with time complexity $\mathcal{O}(\log|\mathcal{R}|)$ and cost computation with time complexity $\mathcal{O}(|\mathcal{M}|)$ are computed. Finally, the time complexity

TABLE II
NoC CONFIGURATIONS

NoC Type	Abbr.	Description
SMART	S	The SMART NoC proposed in [2].
SSR-Net	SSR	The SMART NoC with pre-SSR Network [3].
SHARP	SP	The propapataion-based SSR arbitration [5].
ArSMART	A	Our proposed NoC.

TABLE III
DEFAULT CONFIGURATIONS OF ROUTING ALGORITHM

Routing Algorithm	Abbr.	Classification	Required Info.
XY	xy	Deterministic	r_{src}, r_{dst}
Contention-aware[7]	O	Deterministic	r_{src}, r_{dst}, m , q
General Case	R1	Adaptive	$r_{src}, r_{dst}, m $
Time-triggered Case	R2	Adaptive	r_{src}, r_{dst}, m , q

is $\mathcal{O}(|\mathcal{R}|(\log|\mathcal{R}| + |\mathcal{M}|))$. For the second routing algorithm, the time complexity mainly depends on its route computation algorithm. For the Dijkstra algorithm optimized by the binary heap, the time complexity is $\mathcal{O}(|\mathcal{R}|\log|\mathcal{R}|)$. Thus, our proposed algorithm can be solved in polynomial time. Since NoC size is limited and route computation starts after task mapping and before transmission, it is feasible for route computation to be completed before data transmission. However, the case in which route computation takes a longer time than task computation exists. The route computation would compute a default route, i.e., XY route in our design, at the beginning. In this case, the default simple XY route is returned as the result. We do not prove that our algorithms are deadlock free. However, even if the deadlock occurs during the link arbitration, the controller can stop it by integrating the deadlock detection algorithm [16]. We should note that, users can design their own route computation algorithm to minimize the delay caused by contention and maximize resource utilization.

V. EXPERIMENTAL EVALUATION

A. Experimental Setup

To verify the advantages of our design, we conduct experiments to compare ArSMART NoC with SMART NoC and our algorithms with other routing solutions for SMART NoC. The NoC designs we considered in this article are shown in Table II. Although novel designs revise the original SMART [3], [4], [5] to reduce the overhead, e.g., area and energy, latency is not improved or even worse than the original design. Thus, we set the original SMART as the baseline in experiments except for overhead analysis. For the routing algorithm, we choose the widely applicable XY routing and the start-of-the-art contention-aware routing algorithm proposed in [7]. This routing algorithm is implemented at the design time and needs the support of 2D SSR. Also, additional overhead should be added but we consider the ideal case without overhead here. The configurations of routing algorithms are listed in Table III. The default mapping algorithm is the state-of-the-art contention-aware mapping proposed in [6].

Since no central controlled NoC simulator is available, to verify the functionality and correctness of the micro-architectural component, we implement our NoC design in

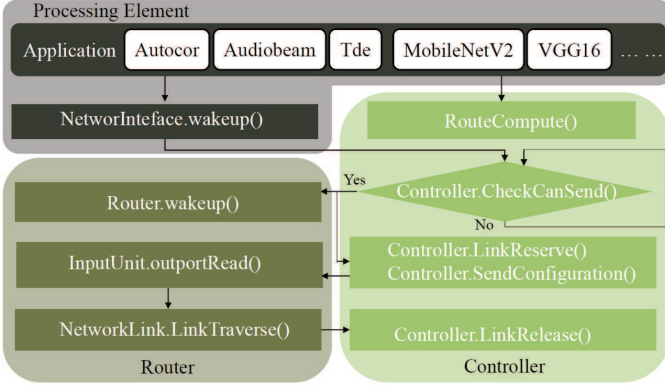


Fig. 8. ArSMART NoC implementation abstract

TABLE IV
DEFAULT CONFIGURATIONS OF NOC SYSTEM

Parameter	SMART NoC	ArSMART NoC
Topology	2D Mesh	2D Mesh
NoC Size	8×8	8×8
Cluster Size	-	8×8
HPC_{max}	8	8
Flit Width	128-bit	128-bit
Package Size	4 flits	4 flits
Buffer Size	4 flits	-
VCs	2 VCs/port	-
Router Pipeline	Three-stage	-
Controller	-	10MB
L1 & D Cache	Private, 32KB	Private, 32KB
L2 Cache	Shared, 512KB/bank	Shared, 512KB/bank
Frequency	1 GHz	1 GHz
Technology	22 nm	22 nm

Gem5 [8], which provides a simulation kernel. As mentioned before, the router is redesigned and the cluster controller is functionally proposed. The main router and controller parts are depicted in Fig. 8. The dependency between each component is represented by the arrow. The route of the message is computed by the controller. As long as the transmission data is prepared in the PE's network interface (NI), the controller begins to arbitrate links for messages. If all links are available, the controller would reserve the link for this message and send configuration information to corresponding routers. Also, the routers along the route would be woken up and configured after receiving the configuration from the controller. Then, data traverses the link from the source to the destination. Finally, the controller releases the resources after transmission completion and lets them be available for other transmissions.

Our router class is derived from the original Gem5 router class, and thus, features of the Gem5 network are still available in our design, i.e., the network topology is configurable and interconnect bandwidth is changeable. However, since the intermediate router buffer is eliminated in our design, the buffer size configuration is disabled. The parameter setting for our experiments is shown in Table V-A. Gem5 records every event in every cycle. Combined with the energy consumption of each event simulated using Hspice in the 22-nm library, we accumulate the NoC energy consumption.

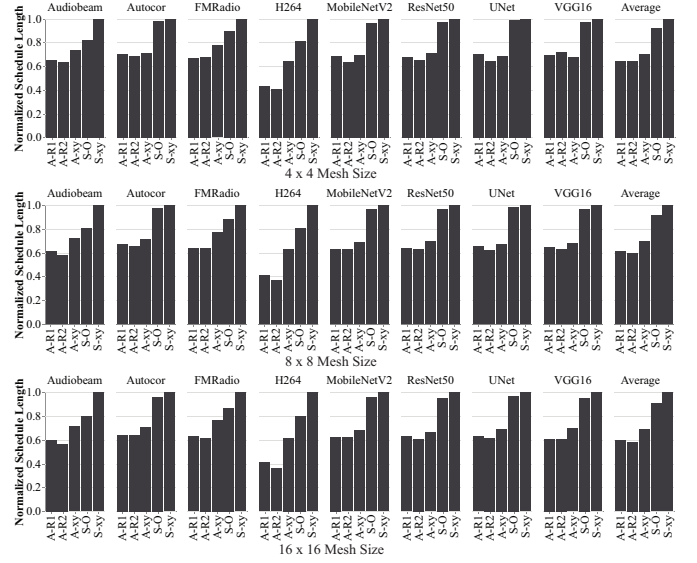


Fig. 9. NoC performance comparison in terms of normalized total schedule length.

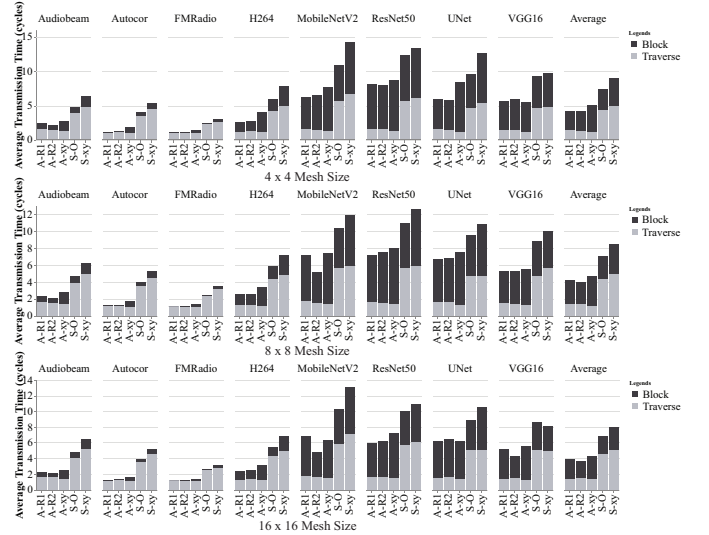


Fig. 10. NoC performance comparison in terms of average transmission latency.

B. Evaluation Results for Real Applications

Together with SMART NoC implemented using Gem5, we analyze ArSMART NoC performance using different metrics. Since the algorithm O and R2 need the information of execution time, we perform testing on a variety of streaming applications as well as AI applications, which have few branches and uncertainty during the execution. Streaming application task graphs are generated from StreamIt benchmark [17] and tasks are mapped using the algorithm proposed in [6]. AI applications and their mappings are generated using Maestro [18], which maximizes data reuse to decrease data movement. The cluster size for 4×4 , 8×8 and 16×16 NoC is 4×4 , 8×8 and 8×8 in this section, respectively.

• **Schedule Length.** Fig. 9 shows the schedule length comparison for different applications. On average, our approach reduces 34.1%, 39.2% and 40.7% total schedule length over SMART NoC for 4×4 , 8×8 and 16×16 NoC size using R1.

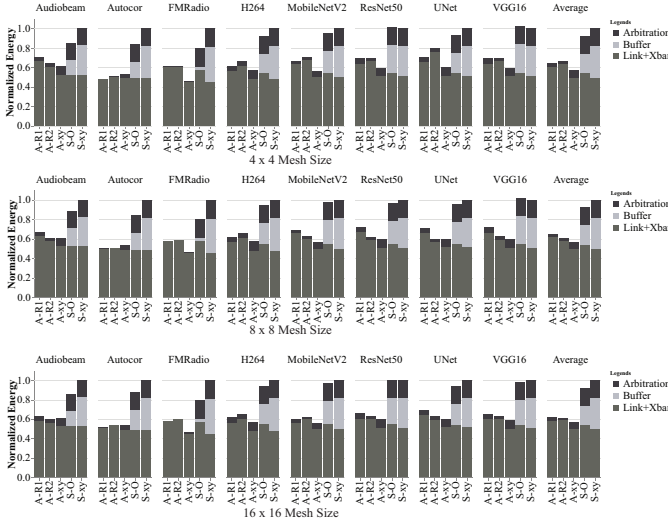


Fig. 11. NoC performance comparison in terms of normalized total energy.

The performance of A-R1 and A-R2 are very close, indicating that our general algorithm is also efficient but can be used in a wider range. Meanwhile, our method dramatically reduces L_{conf} and L_{cs} , resulting in performance improvement. With the increment of NoC size, such the improvement becomes more obvious since that more link resources can be used to establish a long-range path. By comparing the results of S-xy and A-xy, since these two different NoCs use the same routing algorithm, we can roughly get the hardware improvement. We should note that such improvement is not very precise since the scheduling order changes for different cases. The remaining improvement is contributed by the routing algorithm. Our technique outperforms SMART NoCs slightly on AI applications, relatively, whose task graphs are too complicated. However, thanks to the quick configuration process, we achieve at least 12.2% of latency reduction over SMART NoC.

- **Average network latency.** In order to break down the performance gain, we conduct experiments for average network latency shown in Fig. 10. The trend of average network latency is similar to schedule length. Generally, L_{conf} is just a few clock cycles and only counts in message level rather than package level. For the contention delay, our method eliminates the contention at intermediate routers. An additional delay at the source L_{cs} is considered. Using our routing strategies, L_{cs} can be decreased. By comparing the blocking time for A-O, S-R1 and S-R2, we conclude that both of our algorithms are efficient.

- **Energy.** Energy consumption, presented in Fig. 11, of our NoC is much less than SMART NoCs using XY routing. On average, our design reduces 25.3%, 27.4% and 29.7% energy consumption over SMART NoC for 4×4 , 8×8 and 16×16 NoC size, using R1. The energy deduction mainly comes from the removed buffering and decreased arbitration in message level rather than package level. However, since our routing algorithms adopt the arbitrary-turn route which may be longer than the route XY routing chooses, the A-R1 and A-R2 consume more energy on link and crossbar traversal than A-xy and S-xy.

- **AIR.** With the increment of application injection rate (AIR),

TABLE V
DEFAULT PARAMETER SETTINGS FOR SYNTHETIC TRAFFICS

Parameter	Default	Parameter	Default
Number of Nodes	100	Number of Links	300
Avg. Task Volume	8192	Avg. Message Size	8192
Heterogeneity Degree	1	Mesh Size	8×8
Package Size	10 flits	Mapping Algorithm	[6]

shown in Fig. 12, the application schedule length is increased. We can observe that the increment of total schedule length is relatively slow using our approach. In particular, in the case of heavy congestion, performance improvement is obvious for our proposed routing strategies. This shows that our routing strategies always select a route with less contention according to network state.

C. Evaluation Results for Synthetic Traffics

To further explore the advantages and limitations of ArSMART NoC, we generate several random task graphs. Default parameters for these task graphs are listed in Table V.

- **Distance.** In this experiment, we manipulate the task mapping algorithm to change the average distance between the source and the destination PEs from 1 to 5. Fig. 13(a) shows our NoC is scarcely influenced by the distance while SMART NoC latency notably increases. The reason for this result may be that the longer path SMART NoC wants to establish, the more possible this transmission would encounter the interruption by other messages. We can conclude that our proposed design is not distance sensitive, which allows the transmission with long-distance to have the same performance as the transmission between adjacent routers.

- **Message Size.** ArSMART NoC establishes the path in the message level rather than packet level so that the overhead for path establishment is amortized. Thus, the configuration time saving is more obvious for large message sizes. However, for the SMART NoC, the path configuration is conducted at the packet level, the configuration overhead is consistent for each packet, which means that the SMART NoC can process short messages more efficient than ArSMART NoC. To explore the message size with whom the ArSMART NoC can outperform the SMART NoC, in this experiment, we change the number of packets for each message and make the average message size change from 1 to 4. Fig. 13(b) shows the results for task graphs with task execution time equals to 1 and message size varies from 1 to 4. The regression result shows that our ArSMART NoC has a better performance for task graphs with the average message size larger than 1.67. However, we should note that this is not an accurate conclusion due to the influence of schedule orders.

- **Heterogeneity Degree.** In previous experiments, the PEs are homogeneous and their processing rate are the same. For such platform, the contention-aware mapping algorithm is efficient since the objective can be transmission time minimization only. However, in the heterogeneous system, the problem becomes complex since the execution time should be taken into consideration, too. In such case, using mapping algorithms to optimize execution and routing to minimize the transmission is an efficient method to decrease overall schedule length.

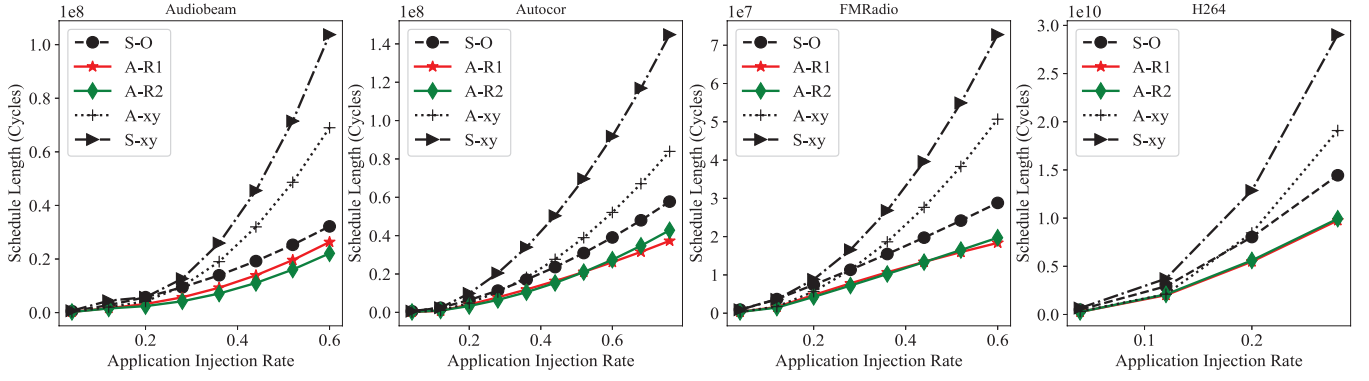


Fig. 12. Schedule length comparison with different application injection rates.

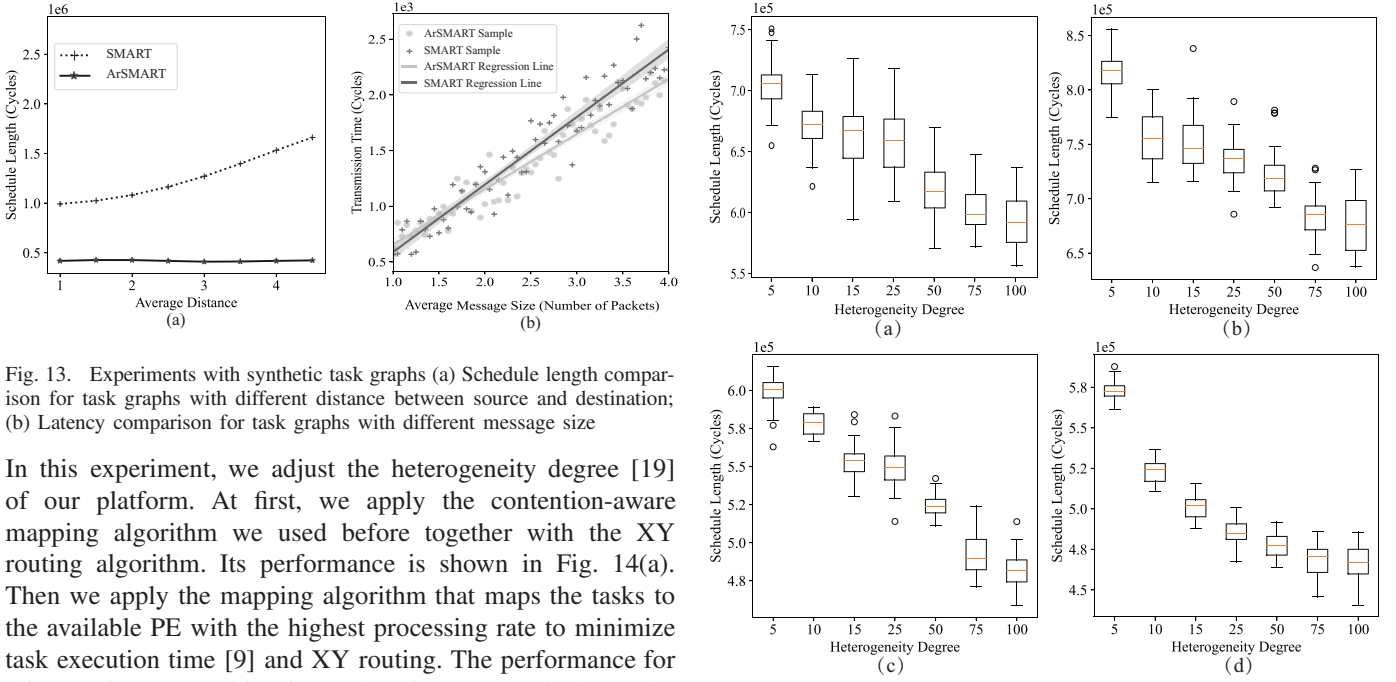


Fig. 13. Experiments with synthetic task graphs (a) Schedule length comparison for task graphs with different distance between source and destination; (b) Latency comparison for task graphs with different message size

In this experiment, we adjust the heterogeneity degree [19] of our platform. At first, we apply the contention-aware mapping algorithm we used before together with the XY routing algorithm. Its performance is shown in Fig. 14(a). Then we apply the mapping algorithm that maps the tasks to the available PE with the highest processing rate to minimize task execution time [9] and XY routing. The performance for this case is presented in Fig. 14(b). Fig. 14(c) and (d) use the same mapping algorithm as (b) but apply our proposed routing algorithm R1 and R2. With the increment of heterogeneity degree, the schedule length for all cases decreases, due to the average processing rate of all PEs increases. However, the last two cases have less schedule length compared with the former two cases. Also, the divergence of the case (c) and (d) are less. This shows that the arbitrary-turn route has stable performance improvement. Through this experiment, we emphasize the importance of using arbitrary-turn route to optimize transmission performance.

D. Overhead Analysis

In this section, we compare ArSMART to original SMART and improved SMART designs, SSR-Net [3] and SHARP NoC [5], in terms of area and power. All of these NoCs apply the 2D configuration. The SMART suffers from high overhead issues since each router must consider all SSRs from upstream routers. At most $HPC_{max}(2HPC_{max} - 1)$ SSRs at each input port are needed, which largely increases wire and arbitration logic area as well as power consumption. SSR-Net, in which an auxiliary SSR network is used, significantly reduces the wire area. Based on this design, SHARP NoC is proposed

Fig. 14. Performance analysis with different task graphs (a) Contention-aware mapping with XY routing; (b) Computation-aware mapping with XY routing; (c) Computation-aware mapping with R1 routing; (d) Computation-aware mapping with R2 routing.

to eliminate the quadratic arbitration by the propagation-based SSR arbitration mechanism. The tool we used, called DSENT [20], for router area and power estimation is the same as [3], [5] for a fair comparison. The technology class we used in DSENT is 22nm. The storage overhead for SMART, SHARP and SSR is the overhead for the buffer, while for ArSMART is the delay register. Since the message arbitration is performed in the controller rather than the router, the arbitration overhead of ArSMART includes the decoding and configuration overhead.

• **Power.** In Fig. 15(a) the router dynamic power for ArSMART, SHARP, SMART and SSR with traffic load of low, medium and high are shown. In this experiment, the $HPC_{max} = 6$ is applied since this is the best achievable values for SHARP under our proposed system configuration. When the traffic load is low, ArSMART reduces about 68% of the power consumption compared with the original SMART design. With the increment of traffic load, the buffer and

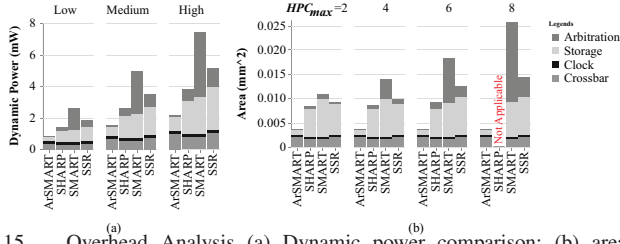


Fig. 15. Overhead Analysis (a) Dynamic power comparison; (b) area comparison.

arbitration power consumption becomes more dominating. Thanks to our “blocking at source” design, the power of storage is greatly reduced. The simplified router design helps ArSMART reduce the arbitration overhead. Under the high traffic load condition, our design can reduce about 70% of power over SMART NoC.

• **Area.** Finally, the area overhead is analyzed. In Fig. 15(b) the router area for SHARP, ArSMART, SMART and SSR with respect to $HPC_{max} = 2, 4, 6, 8$ are shown. Since up to $HPC_{max}(2HPC_{max} - 1)$ SSRs need to be arbitrated in every port for SMART and SSR design, the quadratic increment in arbitration area for these two cases is observed accordingly. Although SHARP decreases arbitration overhead obviously, it cannot support high HPC_{max} . The maximum HPC_{max} SHARP support is only 6. Since in Our ArSMART, the control plane and data plane are separated, the arbitration control is relatively low compared with the other distributed SMART designs (i.e., SMART, SSR, SHARP). Also, our arbitration overhead is not scaled up with the increment of HPC_{max} . Moreover, since in our design, only one delay register is needed for each port, the buffer area is also decreased. The router area overhead of ArSMART is 2.6x-6.8x the original SMART.

VI. RELATED WORKS

In this section, we discuss related NoCs designs to reduce latency, improve energy efficiency or decrease area overhead.

• **SMART NoC.** SMART NoC [2], [21], [22] is proposed to reduce the end-to-end latency by enabling single-cycle multi-hop traversal. In [3], a control network was proposed to reduce wire and energy overhead of the original SMART NoC. Generally, this solution reduces L_{head} but L_{ct} has not been solved effectively. Moreover, extra arbitration may be added for bypassing signals. The most advanced SMART design, SHARP NoC [5], is proposed to eliminate the quadratic arbitration by the propagation-based SSR arbitration mechanism.

• **SDNoC.** To support arbitrary-turn routing which has no constraints on routing decision, software-defined NoC (SDNoC) design has been proposed in [23]. However, these approaches focus on updating the flow table of the router, which increases the complexity of the arbitration dramatically. Finally, it may decrease L_{ct} by adopting excellent contention minimize algorithm we mentioned before, but t_r increased so that the overall performance is degraded. Software-defined circuit switching NoC [24], [25], [26], [27] uses the controller to configure the transmission route. However, these researches use additional packet switching to transmit data packets when there is no path in SDNoC and apply hop-by-hop configuration and transmission, adding additional overhead to this design.

TABLE VI
NoC COMPARISON

NoC	Low latency Bypass	Low A-route Cost	High Adaptability	High Generality
Traditional	×	×	×	✓
SMART	✓	×	×	✓
SDN	×	✓	×	✓
Bufferless	×	×	✓	✓
App. Specific	✓	×	×	×
Our ArSMART	✓	✓	✓	×

• **Bufferless NoC.** On-chip router buffers put pressure on the area and power constraints for NoC. Research [28] shows that 22% of router power is consumed by network buffering resources. [29] describes new algorithms to route packets without buffering. By controlling the injection rate and deflecting flits to undesired ports, buffers can be eliminated. In [30], SCARAB shows a single-cycle bufferless router design. Together with a processor-side buffered router, it reduces the possibility of packet drops and re-transmission costs. Improved bufferless router designs [31], [32] have been proposed. However, since no buffer can temporarily hold packets, packets in bufferless-routing have to keep moving in the links. This may cause additional latency overhead.

• **Application-specific NoC.** Application-specific NoCs [33], [34], [35] generate NoCs in accordance with the application’s communication graph that is known apriori. For AI applications, the novel NoC design [36] is proposed to boost communication performance for spatial neural network accelerator is presented. However, fixed NoC architecture cannot benefit all kinds of applications. Such configurable NoC does not support dynamic change in the run-time, which means the transmission pattern change cannot be handled in this model. However, the traffic during the run-time is not static; it varies phase by phase and is dependent on the mapping of the dataflow over PEs, and the input parameters.

The aforementioned approaches use different technologies and have their specific benefits, as we list in Table VI. We compare them in four metrics, low latency, low cost (i.e., power and area), high adaptability and high adaptability. As we can see from the table, these techniques cannot dominate with each other regarding these costs and benefits. Bypassing intermediate routers (i.e., SMART NoC) and applying routing algorithms with arbitrary-turn (i.e., SDNoC), “A-route” for simplicity, to get low latency needs additional control network, which let the energy consumption increased. The methods with low hardware cost (i.e., Bufferless NoC) cannot meet the latency constraints. The application-specific NoC, denoted as “App. Specific” in the table, which designs NoC by adding additional links at the design time is hard to develop and adapt for software updates. Also, this method cannot handle the transmission pattern change during the run-time.

VII. CONCLUSION

In this article, we proposed an NoC design, ArSMART NoC, which supports single-cycle long-distance data transmission among many cores. Using a cluster-based control method, ArSMART NoC supports any arbitrary-turn route which can

decrease contentions. By configuring the routers directly, we presented a method to setup arbitrary-turn routes from a source to a destination within a very small number of cycles. We also introduced routing algorithms to further decrease communication contention. Compared with the high-performance SMART NoC, we have decreased 40.7% application schedule length and 29.7% in energy consumption on average. Thanks to the simplified buffer and arbitration components, our design reduced the router area and power consumption compared with the start-of-art overhead-aware SMART NoC designs. In the current work, we demonstrate the software design of the controller. Considering the high energy efficiency and performance provided by ASIC, we plan to design specific hardware to implement and accelerate the function of the ArSMART controller.

ACKNOWLEDGMENTS

This work is partially supported by the Ministry of Education, Singapore, under its Academic Research Fund Tier 2 (MoE2019-T2-1-071) and Tier 1 (MoE2019-T1-001-072), and Nanyang Technological University, Singapore, under its NAP (M4082282) and SUG (M4082087).

REFERENCES

- [1] L. Yavits, A. Morad, and R. Ginosar, "The effect of communication and synchronization on amdahl's law in multicore systems," *Parallel Computing*, vol. 40, no. 1, pp. 1–16, 2014.
- [2] T. Krishna, C.-H. O. Chen, W. C. Kwon, and L.-S. Peh, "Breaking the on-chip latency barrier using smart," in *2013 IEEE 19th International Symposium on High Performance Computer Architecture (HPCA)*. IEEE, 2013, pp. 378–389.
- [3] X. Chen and N. K. Jha, "Reducing wire and energy overheads of the smart noc using a setup request network," *IEEE Transactions on Very Large Scale Integration (VLSI) Systems*, vol. 24, no. 10, pp. 3013–3026, 2016.
- [4] I. Pérez, E. Vallejo, and R. Beivide, "Smart++ reducing cost and improving efficiency of multi-hop bypass in noc routers," in *NOCS*, 2019, pp. 1–8.
- [5] Y. Asgari and B. Lin, "Smart-hop arbitration request propagation: Avoiding quadratic arbitration complexity and false negatives in smart nocs," *ACM Trans. Des. Autom. Electron. Syst.*, vol. 24, no. 6, Oct. 2019. [Online]. Available: <https://doi.org/10.1145/3356235>
- [6] L. Yang, W. Liu, P. Chen, N. Guan, and M. Li, "Task mapping on smart noc: Contention matters, not the distance," in *DAC*, 2017, pp. 1–6.
- [7] P. Chen, W. Liu, M. Li, L. Yang, and N. Guan, "Contention minimized bypassing in smart noc," in *2020 25th Asia and South Pacific Design Automation Conference (ASP-DAC)*, 2020, pp. 205–210.
- [8] N. Binkert, B. Beckmann, G. Black, S. K. Reinhardt, A. Saidi, A. Basu, J. Hestness, D. R. Hower, T. Krishna, S. Sardashti *et al.*, "The gem5 simulator," *ACM SIGARCH computer architecture news*, vol. 39, no. 2, pp. 1–7, 2011.
- [9] P. K. Hölzenspies, T. D. ter Braak, J. Kuper, G. J. Smit, and J. M. Hurink, "Run-time spatial mapping of streaming applications to heterogeneous multi-processor systems," *International journal of parallel programming*, vol. 38, no. 1, pp. 68–83, 2010.
- [10] W. J. Dally and B. P. Towles, *Principles and practices of interconnection networks*. Elsevier, 2004.
- [11] S. Park, T. Krishna, C.-H. Chen, B. Daya, A. Chandrakasan, and L.-S. Peh, "Approaching the theoretical limits of a mesh noc with a 16-node chip prototype in 45nm soi," in *Proceedings of the 49th Annual Design Automation Conference*, 2012, pp. 398–405.
- [12] R. Ravindran, C. M. Krishna, I. Koren, and Z. Koren, "Scheduling imprecise task graphs for real-time applications," *International Journal of Embedded Systems*, vol. 6, no. 1, pp. 73–85, 2014.
- [13] J.-S. Shen, *Dynamic Reconfigurable Network-on-Chip Design: Innovations for Computational Processing and Communication: Innovations for Computational Processing and Communication*. IGI Global, 2010.
- [14] A. Silberman and T. J. Marlowe, "A task graph model for design and implementation of real-time systems," in *Proceedings of ICECCS'96: 2nd IEEE International Conference on Engineering of Complex Computer Systems (held jointly with 6th CSESAW and 4th IEEE RTAW)*. IEEE, 1996, pp. 432–441.
- [15] W. Steiner, "An evaluation of smt-based schedule synthesis for time-triggered multi-hop networks," in *RTSS*. IEEE, 2010, pp. 375–384.
- [16] T. Mak, F. Xia, A. Yakovlev, M. Palesi *et al.*, "Embedded transitive closure network for runtime deadlock detection in networks-on-chip," *IEEE Transactions on Parallel and Distributed Systems*, vol. 23, no. 7, pp. 1205–1215, 2011.
- [17] W. Thies and S. Amarasinghe, "An empirical characterization of stream programs and its implications for language and compiler design," in *2010 19th International Conference on Parallel Architectures and Compilation Techniques (PACT)*. IEEE, 2010, pp. 365–376.
- [18] H. Kwon, M. Pellauer, and T. Krishna, "Maestro: an open-source infrastructure for modeling dataflows within deep learning accelerators," *arXiv preprint arXiv:1805.02566*, 2018.
- [19] S. Ali, H. J. Siegel, M. Maheswaran, and D. Hensgen, "Task execution time modeling for heterogeneous computing systems," in *Proceedings 9th Heterogeneous Computing Workshop (HCW 2000)(Cat. No. PR00556)*. IEEE, 2000, pp. 185–199.
- [20] C. Sun, C. O. Chen, G. Kurian, L. Wei, J. Miller, A. Agarwal, L. Peh, and V. Stojanovic, "Dsnet - a tool connecting emerging photonics with electronics for opto-electronic networks-on-chip modeling," in *2012 IEEE/ACM Sixth International Symposium on Networks-on-Chip*, 2012, pp. 201–210.
- [21] C.-H. O. Chen, S. Park, T. Krishna, S. Subramanian, A. P. Chandrakasan, and L.-S. Peh, "Smart: A single-cycle reconfigurable noc for soc applications," in *2013 Design, Automation & Test in Europe Conference & Exhibition (DATE)*. IEEE, 2013, pp. 338–343.
- [22] T. Krishna, C.-H. O. Chen, S. Park, W.-C. Kwon, S. Subramanian, A. P. Chandrakasan, and L.-S. Peh, "Single-cycle multihop asynchronous repeated traversal: A smart future for reconfigurable on-chip networks," *Computer*, vol. 46, no. 10, pp. 48–55, 2013.
- [23] L. Cong, W. Wen, and W. Zhiying, "A configurable, programmable and software-defined network on chip," in *2014 IEEE Workshop on Advanced Research and Technology in Industry Applications (WARTIA)*. IEEE, 2014, pp. 813–816.
- [24] M. Ruaro, H. M. Medina, and F. G. Moraes, "Sdn-based circuit-switching for many-cores," in *2017 IEEE Computer Society Annual Symposium on VLSI (ISVLSI)*. IEEE, 2017, pp. 385–390.
- [25] M. Ruaro, N. Velloso, A. Jantsch, and F. G. Moraes, "Distributed sdn architecture for noc-based many-core socs," in *Proceedings of the 13th IEEE/ACM International Symposium on Networks-on-Chip*, 2019, pp. 1–8.
- [26] M. Ruaro, H. M. Medina, A. M. Amory, and F. G. Moraes, "Software-defined networking architecture for noc-based many-cores," in *2018 IEEE International Symposium on Circuits and Systems (ISCAS)*. IEEE, 2018, pp. 1–5.
- [27] S. Ellinidou, G. Sharma, J.-M. Dricot, and O. Markowitch, "A sdn solution for system-on-chip world," in *2018 Fifth International Conference on Software Defined Systems (SDS)*. IEEE, 2018, pp. 14–19.
- [28] Y. Hoskote, S. Vangal, A. Singh, N. Borkar, and S. Borkar, "A 5-ghz mesh interconnect for a teraflops processor," *IEEE micro*, vol. 27, no. 5, pp. 51–61, 2007.
- [29] T. Moscibroda and O. Mutlu, "A case for bufferless routing in on-chip networks," in *Proceedings of the 36th annual international symposium on Computer architecture*, 2009, pp. 196–207.
- [30] M. Hayenga, N. E. Jerger, and M. Lipasti, "Scarab: A single cycle adaptive routing and bufferless network," in *2009 42nd Annual IEEE/ACM International Symposium on Microarchitecture (MICRO)*. IEEE, 2009, pp. 244–254.
- [31] T. Picornell, J. Flich, C. Hernández, and J. Duato, "Dcnoc: A delayed conflict-free time division multiplexing network on chip," in *Proceedings of the 56th Annual Design Automation Conference 2019*, 2019, pp. 1–6.
- [32] P. Wang, S. Niknam, S. Ma, Z. Wang, and T. Stefanov, "Surf-bleed: A confined-interference routing for energy-efficient communication in nocs," in *Proceedings of the 56th Annual Design Automation Conference 2019*, 2019, pp. 1–6.
- [33] C. Jackson and S. J. Hollis, "Skip-links: A dynamically reconfiguring topology for energy-efficient nocs," in *2010 International Symposium on System on Chip*. IEEE, 2010, pp. 49–54.
- [34] M. Modarressi, A. Tavakkol, and H. Sarbazi-Azad, "Virtual point-to-point connections for nocs," *IEEE Transactions on Computer-Aided Design of Integrated Circuits and Systems*, vol. 29, no. 6, pp. 855–868, 2010.

- [35] K. Sewell, R. G. Dreslinski, T. Manville, S. Satpathy, N. Pinckney, G. Blake, M. Cieslak, R. Das, T. F. Wenisch, D. Sylvester *et al.*, “Swizzle-switch networks for many-core systems,” *IEEE Journal on Emerging and Selected Topics in Circuits and Systems*, vol. 2, no. 2, pp. 278–294, 2012.
- [36] H. Kwon, A. Samajdar, and T. Krishna, “Rethinking nocs for spatial neural network accelerators,” in *2017 Eleventh IEEE/ACM International Symposium on Networks-on-Chip (NOCS)*. IEEE, 2017, pp. 1–8.